

## Chapter 2

# General Kinetic Description of Electrochemical Interfaces

This chapter introduces basic notions concerning the mathematical description of interfacial processes at electrified interfaces [60], the occurrence of electrochemical temporal instabilities as well as the description of spatial coupling effects in electrochemical systems.

### 2.1 State equations of the interface

The study of a physical phenomenon often leads to the elaboration of a model. One looks for a model that is an appropriate representation, often mathematical, of a phenomenon and which captures the essential features of the real system under study. The purpose of such a model is many-fold: First, it can reproduce (ideally all) the facts discovered experimentally, it can help predict the experimental system behavior under various conditions what thereafter (hopefully) can be experimentally verified and, finally and maybe most importantly, it helps rationalize the observed facts within the model's categories of description. Models often deal with the very structure of a system, but it can also be useful to elaborate models of the 'input-output' type which describe the system behavior with respect to its environment.

The aim of an electrochemist is to identify the processes occurring at the electrified interface between a working electrode and the electrolyte, either by elaborating a model for the interface behavior or by trying to find value of some parameters of the system of interest when the reaction mechanism involved is already known. However, in some practical cases, empirical relationships are sufficient.

At this point, some comments on basic concepts regarding the structure of the interface [48] are appropriate. Fig. 2-1 illustrates the generally accepted Stern model of the electrified interfacial region, called the double layer. Charged unsolvated or solvated ions are adsorbed close at the electrode (compact or Helmholtz layer) shielding some of the electric field which extends into the solution; furthermore within some distance from the surface, called the diffuse layer, excess ions are found according to a Boltzmann distribution. The compact layer is further subdivided by the plane

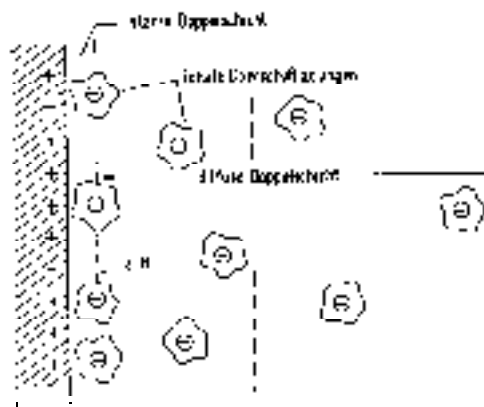


Figure 2-1: Illustration of the compact (several Angstrom in width = radius of solvated ions) and the diffuse double layer the width of which depends on ionic strength of the solution (10 - 100 Angstrom). ä.H.= outer Helmholtz plane.

of closest approach for the centers of the ions which are nonspecifically adsorbed (outer Helmholtz plane, ä.H. in the figure), i.e. ions which still are surrounded by solvent molecules and by the plane for the centers of specifically adsorbed ions (inner Helmholtz plane, not shown). Beyond the diffuse part of the double layer, bulk concentration conditions and electro-neutrality is assured.

The elaboration of a model for the interface behavior is derived from the general equations of physics that take account of the non-linear character of the processes involved. The spatial distribution of the general state variables  $\phi(r, t)$  and  $c_i(r, t)$  -the electric potential and concentration of species  $i$  at point  $r$  of the electrochemical system and time  $t$  - is determined by a set of differential equations, subject to the appropriate boundary and initial conditions.

$$\nabla^2 \phi = -\rho_c + \nabla \cdot \vec{P} \quad (2.1)$$

$$\frac{\partial c_i}{\partial t} = -\nabla \cdot \vec{J}_i + \xi_i \quad (2.2)$$

where  $1 \leq i \leq m$ .

The first of these coupled  $(m + 1)$  equations generalizes the Poisson equation, where  $\rho_c$  is the electric charge density per unit volume and  $\vec{P}$  the dielectric polarization. The second set of equations generalizes the hydrodynamic equations and applies to the  $m$  types of chemical entities involved in the system;  $c_i$  is either a surface or a bulk concentration,  $\vec{J}_i$  is the flux, and  $\xi_i$  is a term representing the production or consumption of a chemical species  $i$  generally arising from chemical and electrochemical reactions. This last term can be made explicit from the mass balance of the reaction scheme to be tested and from the laws of homogeneous and heterogeneous kinetics.

Starting from this general frame work, the elaboration of a model for the interface will be performed by making a certain number of hypotheses which generally allow

one to simplify the initial equations. This simplifying hypothesis fall into several categories, each of which is now briefly described.

### 2.1.1 Poisson equation versus Laplace equation

The charge density,  $\rho_c$ , in eq. 2.1 can be considered as non-zero in particular situations. Firstly, around a reference ion in the solution, in the Debye-Hückel theory [61]. Secondly, in the Helmholtz part as well as in the diffuse part of the double layer for which a static and dynamic description has been given [61, 48].

In practice, however, it is often assumed that net electric charges within the solution can be neglected and therefore the Laplace equation is a reasonable approximation for the description of the potential distribution in the electrolyte:

$$\nabla^2\phi = 0 \quad (2.3)$$

This is valid for every volume element of the solution, since the electrolyte, as a whole, is electro-neutral, i.e. there are no net sources of charge. Early electrochemical models dealing with the potential distribution within the electrolyte placed emphasis exclusively on gradients perpendicular to the electrode surface. This led to the concept that the ohmic potential drop due to the solution resistance  $R$  must be added to the potential drop right at the interface

$$U = \phi_0 + I_{tot}R \quad (2.4)$$

where  $U$  is the potential drop between the working electrode and the point of the reference electrode by which the potential of the working electrode is controlled.  $\phi_0$ <sup>1</sup> denotes the interfacial potential drop, called the double layer potential, determining the electrochemical processes<sup>2</sup>.  $I_{tot}$  represents the current flowing between the working electrode and the reference electrode. Recall, however, that ideally there is no current actually flowing into the reference electrode; instead, all current is collected by the third electrode of an electrochemical setup, the counter (auxiliary) electrode (see chapter 3). Fig. 2-2 illustrates the potential drops between working and reference electrode. Eq. 2.4 will become crucial as electrochemical instabilities will be discussed.

### 2.1.2 Equations describing the concentration change

The hypothesis often made is that of a dilute solution for which the flux of a species  $i$  can be separated into a flux due to diffusion and a flux due to migration in an electric field [62]. Assuming that the transport properties ( $D_i, \mu_i, u_i$ ) are uniform in

---

<sup>1</sup>Note that the subscript '0' will be dropped in subsequent chapters where no potential inside the solution is concerned.

<sup>2</sup>Note that a further refinement of this statement will be given when double layer effects will be discussed.

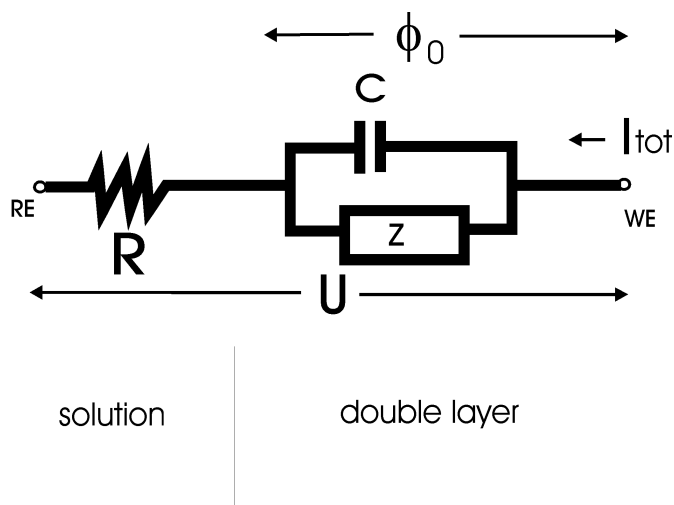


Figure 2-2: General equivalent circuit of an electrochemical cell,  $I_{\text{tot}}$  = total migration current,  $R$  = ohmic electrolyte resistance,  $C$  = double layer capacitance,  $Z$  = faradaic impedance,  $U$  = outer applied potential,  $\phi_0$  = double layer potential.

the solution bulk and independent of the concentration  $c_i$ , the concentration change in the absence of any chemical reaction is given by:

$$\frac{\partial c}{\partial t} = D_i \nabla^2 c_i - \vec{v} \cdot \nabla c_i + z_i F u_i \nabla(c \nabla \phi) \quad (2.5)$$

where  $D_i$  is the diffusion constant of a species  $i$ ,  $\vec{v}$  the velocity field of the liquid,  $u_i$  the mobility of  $i$ ,  $z_i$  its charge number and  $\phi$  the potential as given in eq. 2.3 (see section 1.2). The concentration change is most generally governed by Diffusion (first term), convection (second term) and migration (third term).

If electro-neutrality is assured, in the presence of inert major ionic species in excess (supporting electrolyte), one can neglect the migration terms of the electroactive species. Generally, calculation of concentrations in the presence of convection is difficult unless very special convective conditions hold. The known example of a rotating disc electrode, for instance, gives rise to a constant gradient at the interface. Mostly however, calculation of concentration is simple only if one can neglect convection. This is sufficiently well fulfilled if Schmidt's number (viscosity/diffusion coefficient) is sufficiently high (several thousand). The concentration gradient is then located in the so-called Nernst layer (see chapter 5 and 8) of thickness  $\delta$ , within which the liquid is nearly motionless. The transport equation then reduces with good accuracy to the simple Fick's law of diffusion:

$$\frac{\partial c}{\partial t} = D_i \nabla^2 c_i \quad (2.6)$$

Convection is now taken into account by applying the boundary conditions on  $c_i$ ,

that is  $c_i$  equals its bulk value at a finite distance from the interface instead of at infinity.

### 2.1.3 Separation of the faradaic current from the charging current of the double layer

Strictly speaking, there is close coupling between faradaic currents, i.e. charge transfer due to chemical reactions, and capacitive currents, i.e. charge flowing into the double layer. Still, in most models, in particular at high concentrations of the supporting electrolyte, calculation of the double layer potential is greatly simplified by the hypothesis that a separation between these currents is possible. Then, the overall current is given by:

$$I_{tot} = I_{cap} + I_{far}. \quad (2.7)$$

Eq. 2.7 is particularly important in forthcoming models of electrochemical systems and will serve as the temporal evolution equation for the double layer potential. The equation can equivalently be considered as a charge conservation equation as well as a current balancing equation.

### 2.1.4 Heterogeneous reactions at the interface

In applying laws of heterogeneous chemical kinetics to the adsorbed species involved in electrochemical kinetics, the mass balance equation for a species  $i$  can be written:

$$\frac{\partial c_{i,surface}}{\partial t} = \xi_i + D_{i,surface} \nabla c_{i,surface} \quad (2.8)$$

where  $\xi_i$ , the source term, can be either positive or negative and represents the electrochemical or chemical surface reactions, the adsorption or desorption.  $D_{i,surface}$  is the surface diffusion coefficient of species  $i$ . The surface concentration of  $i$ ,  $c_{i,surface}$ , is generally considered as being proportional to the coverage fraction  $\theta_i$  of the electrode surface by species  $i$

$$c_{i,surface} = \beta_i \theta_i \quad (2.9)$$

where  $\beta_i$  is the maximum surface concentration of  $i$ . By analogy with gas phase adsorption, an expression for the value of  $\theta_i$  is obtained by choosing an isothermal law (isotherm). The shape of the isotherm critically influences the relation between the heterogeneous reaction rate and the volume concentration of species near the double layer.

### 2.1.5 Charge-transfer at the interface

The charge balance gives the faradaic current which is a function of several quantities [48, 63].

The general expression of the rate of charge transfer with fast mass transport reads:

$$I_{far} = I_{far}(c_{bulk}, \phi, T, p, A, \omega) \quad (2.10)$$

with  $c_{bulk}$  being the bulk concentration of  $i$ ,  $T, p$  absolute temperature and pressure,  $A$  the electrode area and  $\omega$  the rotation speed (rotating disc). The most commonly adopted formalism for the description of  $I_{far}$  of a simple electrochemical reaction  $A \rightleftharpoons B + ne^-$ , where  $n$  electrons are exchanged with the electrode, is the Butler-Volmer expression:

$$\frac{I_{far}}{nFA} = c_{A,surface} k e^{\frac{\alpha nF}{RT}(\phi - \phi^0)} - c_{B,surface} k e^{-\frac{(1-\alpha)nF}{RT}(\phi - \phi^0)} \quad (2.11)$$

Here, the surface concentrations  $c_i$ , the rate constant  $k$  and the double layer potential  $\phi$  are related to the observable charge transfer.  $\phi^0$  is the standard potential of the reaction and  $\alpha$  denotes the symmetry factor [48]. In situations where the mass transport is slow the surface concentration  $c_i$  will be different from  $c_{bulk}$ .

### 2.1.6 The Frumkin effect

In a previous section, the splitting of the double layer into a compact part and a diffuse part has been introduced. Equivalently, the total potential drop across the double layer,  $\phi$ , can be subdivided into a portion across the compact layer up to the outer Helmholtz plane and the portion which drops across the diffuse part, called  $\phi_2$  (see Fig.2-3 where the potential in the bulk solution was set to zero). This potential splitting can affect the electrode reaction in two ways. (i) The concentration of the electroactive species at the outer Helmholtz plane will be different from that outside the Nernst diffusion layer due to coulomb interactions. The concentration difference will generally be a function of  $\phi_2$ . (ii) The potential difference driving the electrode reaction is not  $\phi$ , but instead  $(\phi - \phi_2)$ ; thus the effective electrode potential (double layer potential) is  $U - IR - \phi_2$ . Both effects can lead to a non-trivial  $I - \phi$  characteristic of an electrode process. In particular, the rate of charged transfer might decrease with increasing overpotential over some potential interval, when anion reduction or cation oxidation is considered.

## 2.2 Polarisation control

As Fig. 2-2 suggests, the electrochemical system under potentiostatic control can be thought of as an ensemble of an inner circuit (double layer) with faradaic and capacitive currents placed in series with an external circuit (load line) with ohmic resistance  $R$ . This ensemble is characterized by dependent state variables such as current  $I$  and double layer potential  $\phi$  and parameters governed by the experimenter (constraints) such as the outer potential  $U$  between reference and working electrode. In a stationary state the state variables of the external and the internal circuit and the imposed constraint must be matched. Usually, the steady state characteristics is plotted by varying the constraints imposed and by measuring the change of a

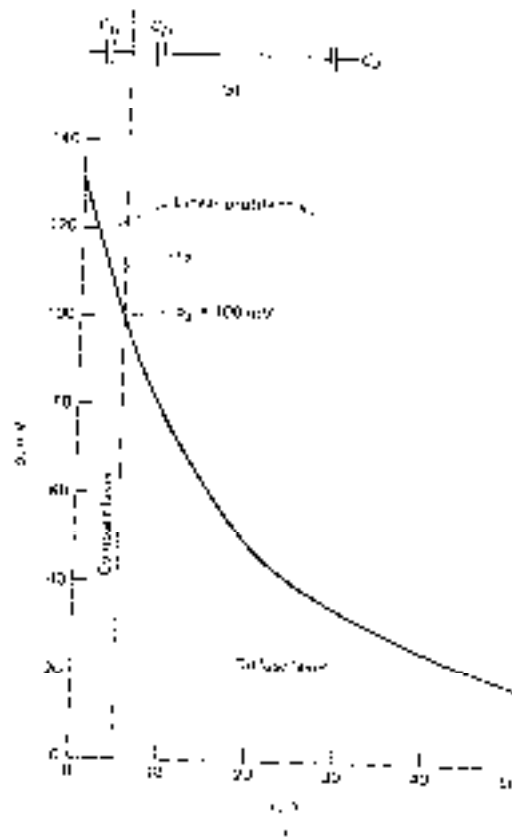


Figure 2-3: (a) The differential capacitance in the Stern model as a series of Helmholtz and diffuse layer capacitances. (b) Spatial profile of potential through the solution side of the double layer (calculated for 0.01 M 1:1 electrolyte in water 25°C).

state variable (e.g.  $I - U$  plots). This technique is called polarisation control. The dependence of state variables and constraints in the load line are essentially captured in eq.2.4. Matching the currents in the steady state leads to

$$I_{far}(c_{bulk}, \phi, T, p, A, \omega) = I_{load} = -\frac{\phi}{R} + \frac{U}{R} \tag{2.12}$$

This relation will help rationalize the occurrence of dynamical instabilities in electrochemical systems. Before the mechanistic origin of instability is introduced, however, the different types of polarisation control need to be discussed.

First, there are polarisation conditions, where the ohmic resistance  $R$  is finite and, consequently,  $\phi$  may be different from the fixed outer potential  $U$ ; such conditions are called *potentiostatic with fixed outer potential* or simply *potentiostatic* and are

most frequently employed in the upcoming chapters. Secondly, conditions of electrochemical measurements for vanishing ohmic resistance  $R$  are referred to as *truly potentiostatic conditions*, since  $\phi = U = \text{const.}$  In this case, the double layer potential is no longer a state variable, but instead a system parameter.

Finally, if the total current is kept constant, the polarisation conditions are referred to as *galvanostatic*.

## 2.3 Dynamical instabilities at electrochemical interfaces

### 2.3.1 Origin of electrochemical bistable behavior

Consider Fig. 2-4 where the load line and the faradaic polarisation curve are plotted at given constraints  $U$  and  $R$ . In Fig. 2-4a the faradaic process exhibits a normal positive regulation over the entire potential interval. It is seen that there is only one stationary set  $(I, \phi)$  of state variables determining the system behavior. Multiple working points become possible, however, if the stationary faradaic polarisation curve shows a region of inverse regulation (negative faradaic impedance  $Z = \frac{dI_{far}}{d\phi}$  or equally negative differential resistance, N-shaped polarisation curve) as given in Fig. 2-4b and c. According to Koper [64] the origin of a region of negative impedance can be rationalized as follows: since the faradaic current is given according to

$$I_{far} = nFAck e^{\beta\phi}$$

for the impedance follows

$$\frac{dI_{far}}{d\phi} = nF \frac{dA}{d\phi} c k e^{\beta\phi} + nFA \frac{dc}{d\phi} k e^{\beta\phi} + nFAc \frac{dk}{d\phi} e^{\beta\phi}.$$

A N-shaped  $I/\phi$  curve ( $\frac{dI_{far}}{d\phi} < 0$ ) can therefore stem from a Frumkin effect in the double layer ( $\frac{dc}{d\phi} < 0$ ), the potential-dependent ad- and desorption of a catalyst ( $\frac{dk}{d\phi} < 0$ ) or the possibility that the available surface area becomes potential-dependent, e.g. due to fast adsorption processes ( $\frac{dA}{d\phi} < 0$ ). Usually, in the case of three stationary states, two of them are stable whereas the third one is unstable. Upon perturbing the system from one stable stationary state, a transition to the other stable steady state can be achieved without changes in the constraints. Note that the dynamic bistable behavior is determined by the temporal evolution of the double layer only. All chemical species affecting the reaction are assumed to be stationary at all times.

It is obvious from Fig. 2-4 that for bistability to occur apart from the presence of a potential region with negative impedance (= negative differential resistance, NDR), a condition as to the absolute value of the ohmic resistance  $R$  must be fulfilled, namely  $|Z_f| < R$ , where  $Z_f$  is the faradaic impedance. This feature had been conjectured from early on to be critically involved in the instability mechanism [65, 66]

In addition to the electrochemical bistability, an electrochemical system can become bistable due to a purely chemical bistability not involving the double layer potential as essential variable. There are only few known experimental bistable systems of this type [67].



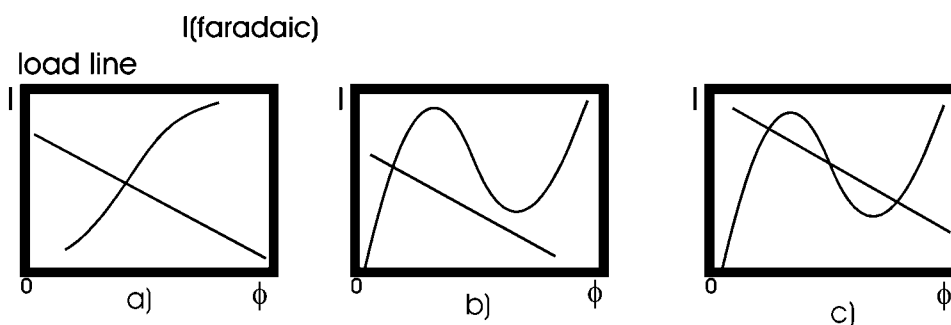


Figure 2-4: The origin of multiple stationary states in electrochemical systems. a) Always one stable steady state. b) and c) Due to an N-shaped stationary polarisation curve, a transition to bistability (three stationary points) can occur.

### 2.3.2 Electrochemical oscillations

Sustained periodic behavior is generally obtained from bistability if an additional slow degree of freedom associated with a slow state variable arises in the system. If the regulation between the bistable part of the system and the additional variable is chosen properly [68, 33, 69] and if the timescales are sufficiently different, the fast positive feedback based on the electrical quantities and the slow negative feedback can interact to yield electrochemical oscillations. As already conjectured in early electrochemical literature the slow negative feedback can result from the rate-determining slow transport of electroactive species leading to variations in the double layer concentration [65, 66, 70, 71, 72]. A general mathematical formulation of the problem together with a thorough analysis of electrochemical oscillations was for the first time given by Koper [73, 64, 74].

Sustained oscillations in current or potential are also conceivable in purely chemical oscillators with one or more reaction steps being associated with charge transfer at the interface. Such oscillators would not involve the double layer potential as an essential variable (truly potentiostatic oscillators).

### 2.3.3 Mechanistic classification of electrochemical oscillators

The first mechanistic classification of oscillatory electrochemical systems has been put forward by Wojtowicz [15] who generally distinguished between purely chemical oscillators with charge transfer and electrochemical oscillators characterized by an interaction of external and internal circuit. More recently, Koper [73, 64, 74, 23] developed a more precise picture as to a possible categorization of electrochemical oscillations: Koper identified the group of oscillators which require both a negative differential resistance and a finite ohmic resistance  $R$  for instabilities. Within this group, he further subdivided into electrochemical oscillators which oscillate only under potentiostatic conditions (with additional external ohmic resistance if the solution resistance is not sufficient) and those which exhibit potential oscillations under galvanostatic con-

ditions as well. According to ref. [27] oscillators of the former and latter type are referred to as "NDR-oscillators" and "HNDR-oscillators", respectively, indicating the requirement of a negative differential resistance. HNDR stands for 'hidden negative differential resistance'. The prominent feature of a HNDR-oscillator is the fact that the differential resistance is negative only on a fast time scale and therefore is not visible in a stationary  $I/U$  curve. The fast time scale can be caused by a fast ad- and desorbing species which blocks free surface sites and thereby leads to a negative  $\frac{dA}{d\phi}$ .

There are numerous experimental examples of these two oscillator classes;  $\text{In}^{3+}$  reduction in the presence of catalysts as well as the reduction of peroxodisulphate in alkaline solution are prominent examples of NDR oscillators, whereas the oscillatory hydrogen oxidation reaction in the presence of UPD metals and adsorbing ions belongs to the latter HNDR type [75, 29]. Koper further pointed out his finding that NDR oscillators usually show the so-called cross-shaped phase diagram (XPD) [44] in two-parameter bifurcation diagrams, whereas HNDR oscillator generally exhibit more complex bifurcation diagrams involving a saddle-loop bifurcation of stable periodic orbits [64, 29, 26]. The shape of these bifurcation diagrams is related to the existence of highly degenerate bifurcation points that cannot occur in systems with a XPD [74]. A systematic study of this phenomenon, in particular the study of the transition between the bifurcation diagrams of the two oscillator classes was still missing.

Furthermore, Koper picked up the concept of purely chemical oscillators referring to them as truly potentiostatic oscillators [23]. These oscillators show sustained periodic behavior even in the limiting case of truly potentiostatic conditions, i.e. where the double layer potential is kept constant without quenching the oscillations. Since the instability is of chemical nature, the classification scheme of chemical oscillatory systems can be applied [33] if a simple synergistic autocatalysis is involved. For more complicated mechanisms of instability (competitive autocatalysis or autocatalysis-free oscillatory instability) classification schemes are still to be elaborated. Note that at higher values of the ohmic resistance,  $\phi$  does in fact oscillate even if it is nonessential for the dynamics. There are a few experimental systems which are believed to fall into this class but clear evidence for the purely chemical nature of their instability is still missing [76, 67, 77, 78]. Consequently, the bifurcation behavior and the impedance spectra of those electrochemical system are poorly investigated both in experiment and theory.

## 2.4 Spatiotemporal description of electrochemical interfaces

So far in this chapter, the kinetic description of an electrified interface considered exclusively spatially homogeneous systems, i.e. systems in which any spatial potential variation was neglected. However, it is well known from studies by Ostwald and Franck[14, 13] that the electrode cannot always be assumed to be spatially homogeneous. As pointed out in chapter 1 for general chemical systems, spatial transport processes may occur parallel to the reactive interface and need to be included as spatial coupling terms into a complete dynamic model description.

Fig. 2-5 reviews the most common types of spatial coupling: A global coupling is defined as one that is felt instantaneously and equally strongly at any spatial position  $x$  of the system. A local coupling, in contrast, implies, that only two points in close distance are coupled, whereas two distant points do not 'feel' each other at all. Finally, a nonlocal coupling is intermediate global and local in the sense that the region of coupling is wider than in the local case, possibly including the entire system, and that the coupling strength between two points varies with their spatial distance. Note that in Fig. 2-5 all spatial points along the electrode are assumed to be subject to the same coupling function. Recent calculations for specific electrode geometries indicate that this is not necessarily the case [40]. Local coupling, e.g. diffusion, as well as global coupling, e.g. through the gas phase in UHV experiments, have been extensively studied in models and experiments and are well understood [79, 80, 57, 59, 56, 58].

Unlike reaction-diffusion systems where spatiotemporal patterns arise from the interaction of an autocatalysis and diffusional coupling, in electrochemical systems an additional transport mechanism occurs through the transport of charged species in an electric potential gradient (migration processes). As pointed out previously, the strong tendency of migration to neutralize net charges within the solution justifies the hypothesis that the potential distribution is governed by the Laplace rather than by the Poisson equation. This assumption is actually the starting point of all recent modeling approaches of spatial electrochemical pattern formation. Furthermore, the presence of migration coupling in electrochemical systems gives rise to peculiar properties absent in reaction-diffusion systems.

Early modeling addressed complex spatial pattern such as waves and antiphase oscillations observed during Ni dissolution in sulfuric acid [81, 34, 82]. Even though there was a correspondence of model and experiments, the numerical results remain questionable due to some unreasonable model assumptions.

A model approach by Koper and Sluyters [83] fails to allow for a nonlinear potential distribution between working and reference electrode which reduces the coupling parallel to the interface across the electrolyte to a formal diffusion. Furthermore, potential inhomogeneities outside the diffusion layer are neglected which is in contrast to experiments [36]. Hence, the latter model approach is also unable to adequately capture the characteristics of electrochemical coupling.

Flätgen and Krischer [84, 85, 86] reported on spatio-temporal phenomena in the bistable or oscillatory regime during peroxodisulphate reduction, a NDR oscillator, at a Ag ring electrode or disk. They found travelling potential fronts along the electrode mediating the transition between the active and passive state. Unlike reaction-diffusion fronts, the electrochemical fronts did not show a constant velocity but exhibited acceleration [85]. Similar accelerating fronts were observed during cobalt electrodisolution [87]. Solving the Laplace equation in two space dimensions  $x$  and  $z$ , corresponding to the direction parallel and respectively perpendicular to the electrode, by means of Fourier modes, Flätgen and Krischer calculated the migration term  $I_{mig}$ , i.e. the potential gradient at the interface in direction of  $z$ , in the charge

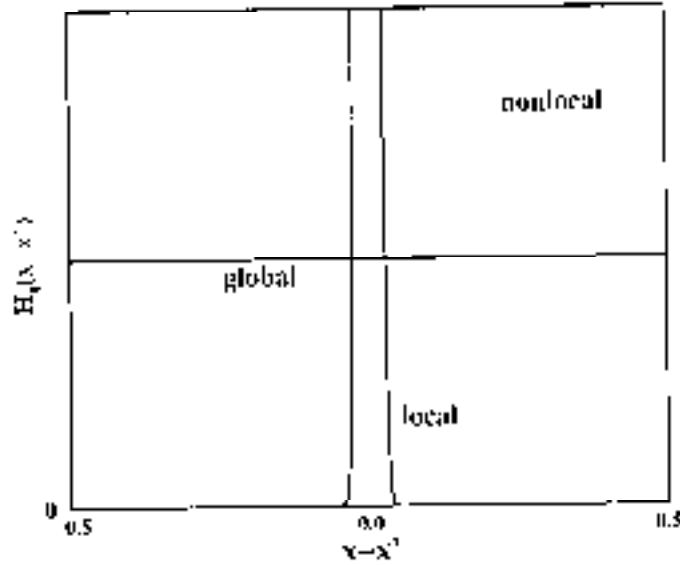


Figure 2-5: Common types of one-dimensional spatial coupling in dynamical systems with periodic boundary conditions.  $H$  denotes the coupling strength,  $(x-x')$  represents the spatial position relative to a reference point  $x'$ .

balance equation [36, 27]

$$C_{dl} \frac{\partial \phi_0(x, t)}{\partial t} = -I_{far} + I_{mig} = -I_{far}(x, t) - \frac{\sigma}{\beta} \frac{\partial \phi(x, t)}{\partial z} \Big|_{interface}. \quad (2.13)$$

It is this equation which governs the time evolution of the interfacial potential (see also eq.2.7) and therefore is the crucial part of the model.  $C_{dl}$  denotes the interface capacity,  $\beta$  is a geometrical parameter and  $\sigma$  is the conductivity of the solution. Simulations using the Flätgen-Krischer model revealed that the presence of a nonlocal coupling across the electrolyte due to migration currents parallel to the electrode must be held responsible for the acceleration [84, 36].

Mazouz et al. [37, 38] further investigated the two-dimensional Flätgen-Krischer model with respect to the range and strength of the spatial coupling. As to the range of the coupling, they stressed the significance of the length scale of the electrochemical system  $\beta$ , i.e. the ratio of the distance between the working electrode and an equipotential plane (reference electrode) and the area of the working electrode, whereas the conductivity was found responsible for the strength of the spatial coupling. Large  $\beta$  were found to increase the range of the coupling, whereas very small  $\beta$  led to diffusion-like coupling.

Christoph, finally, recently suggested an alternative approach to the calculation

of the total migration current  $I_{mig}$  in the charge balance equation. Whereas Flätgen used a Fourier mode representation, Christoph employed theorems on Green's functions in order to develop a numerically tractable formalism for eq. 2.13 even for complex electrode geometries, e.g. requiring mixed boundary conditions [40]. Unlike previous electrochemical models Christoph's approach led to an illustrative integral representation of eq. 2.13 [41]. In the case of periodic boundary conditions along the interface of a ring electrode with a rotational-symmetric point-like reference electrode, eq. 2.13 becomes

$$\frac{\partial \phi_0(x, t)}{\partial t} = F_{local}(x, t) + \int_{ring} H(|x' - x|) (\phi'_0 - \phi_0) dx' \quad (2.14)$$

where the spatial coupling is entirely taken care of by the integral expression containing the coupling function  $H$  and the potential difference of two points ( $\phi'_0 - \phi_0$ ) considered. The function  $H$  represents the coupling between a given reference point  $x$  and the other points along the ring; for the ring geometry considered,  $H$  is identical for all  $x$ , thus depends only on distance ( $x' - x$ ). The function  $F$  includes all local chemical dynamics. Christoph's integral formalism not only allows the precise formulation of a three-dimensional ring geometry including a finite ring width, but also can be used to approach complex geometries such as ribbon or disk electrodes. Generally, in Christoph's formalism the counter electrode is considered to be at infinity.

For the geometry of interest for forthcoming experiments in chapter 6, i.e. periodic boundary conditions in  $x$  direction along a 'quasi one-dimensional' working electrode with point reference electrode on the rotational axis, the dependence of  $H$  on system constraints such as (i) the geometric aspect ratio  $\beta$  of the system and (ii) an external ohmic resistance  $R_{ex}$  in series to the working electrode can be lumped into a single parameter  $B$ :

$$H = H(B)$$

$$B = B(\text{aspect ratio}, R_{ex}).$$

Fig. 2-6 summarizes the predictions of the integral formalism as to the dependence of the sign of  $H$  on the system parameter  $B$ . The system length was normalized to 1 and the reference point considered is located at  $x = 0.5$ . For a large value of the aspect ratio, i.e. a large distance between working and point-like reference electrode, and in the absence of an external ohmic resistance, the value of  $B$  is zero and the  $H$  is given by the middle curve in Fig. 2-6. All points along the ring are coupled positively with the coupling strength decreasing with distance. If the reference electrode is approached towards the center of the ring electrode,  $B$  becomes negative; this leads to a negative offset of  $H$  resulting in a negative nonlocal coupling along the ring electrode, i.e. a positive short-range, but negative long-range coupling, as shown in the lower curve in Fig. 2-6. The negative nonlocal coupling has important consequences as to the dynamical behavior of the system. Whereas two adjacent points tend to synchronize their behavior, two distant points do the

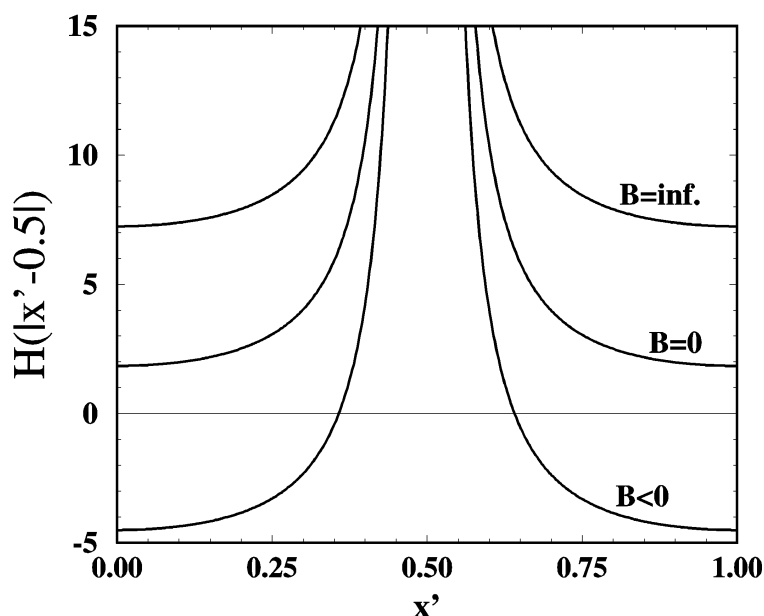


Figure 2-6: Dependence of the coupling function  $H$  on parameter  $B$  for a reference point located at  $x=0.5$ . For large aspect ratios and no external resistance ( $B=0$ ),  $H$  represents a positive nonlocal coupling. For small aspect ratios and no external resistance ( $B$  negative) a negative nonlocal coupling, i.e. a positive short-range and negative long-range coupling, arises. An additional external resistance increases  $B$  which leads to a positive offset of  $H$  until in the galvanostatic limit a strong positive nonlocal coupling exists (adapted from [40]).

opposite. Unlike a negative global coupling, the nonlocality of the negative coupling confines the opposite coupling to a more localized portion of the electrode. If an external resistance is put in series with the working electrode, the value of  $B$  increases leading to a positive offset of the coupling function as shown in the upper curve in Fig. 2-6. In the galvanostatic limit a strong positive nonlocal coupling results which instantaneously tends to synchronize the electrode.

The negative nonlocal character of  $H$  can give rise to qualitatively new dynamical states and phenomena unknown in reaction-diffusion systems. In chapter 6, experimental evidence will be provided in favor of the numerical predictions obtained by Christoph using the integral formalism.